DEFACTO - battery DEsign and manuFACTuring Optimisation through multiphysic modelling

D.4.1

Date: 30/06/2021

This document is the report on a Lattice Boltzmann Method (LBM) model for electrolyte intrusion led by DLR. It contains information of the physical background, implementation, validation and usage of micro- and nanoscopic multi-component flow models for the simulation of electrolyte filling processes.

This project has received funding from the European Union's Horizon 2020 research and innovation programme under grant agreement No 875247.

Horizon 2020
European Union Funding
for Research & Innovation

This project has received funding from
the European Union's Horizon 2020 research and innovation
programme under grant agreement No 875247

Project details

Project acronym	DEFACTO	**Start / Duration**	*01/01/2020 (42 months)*
Topic	LC-BAT-6-2019	**Call identifier**	*H2020-LC-BAT-2019-2020*
Type of Action	RIA	**Coordinator**	*CIDETEC*
Contact persons	*Elixabete Ayerbe*		
Website	www.defacto-project.eu		

Deliverable details

Number	*4.1*		
Title	*Report on a LBM model for electrolyte intrusion*		
Work Package	*WP4*		
Dissemination level	Public	**Nature**	*Report*
Due date (M)	18	**Submission date (M)**	*18*
Deliverable responsible	**DLR**	**Contact person**	***Martin Lautenschläger***

Horizon 2020
European Union Funding
for Research & Innovation

This project has received funding from
the European Union's Horizon 2020 research and innovation
programme under grant agreement No 875247

Deliverable Contributors

	Name	Organisation	Role / Title	*E-mail*
Deliverable leader	Timo Danner	DLR	Project supervisor	*Timo.Danner@dlr.de*
	Martin Lautenschläger		Researcher	*Martin.Lautenschlaeger@dlr.de*
Contributing Author(s)	-			
Reviewer(s)	María Yáñez	CID	Project Coordinator	*myanez@cidetec.es*
	Elixabete Ayerbe	CID	Project Coordinator	*eayerbe@cidetec.es*
Final review and quality approval	María Yáñez	CID	Project Coordinator	*myanez@cidetec.es*

Document History

Date	Version	Name	Changes
28/05/2021	V1	Martin Lautenschläger	First version

Horizon 2020
European Union Funding
for Research & Innovation

This project has received funding from
the European Union's Horizon 2020 research and innovation
programme under grant agreement No 875247

Content

Horizon 2020
European Union Funding
for Research & Innovation

This project has received funding from
the European Union's Horizon 2020 research and innovation
programme under grant agreement No 875247

1 Executive Summary

The current report describes different Lattice Boltzmann models for structurally resolved multi-phase flow in microporous electrode structures. In addition, also a model extension for structurally unresolved multi-phase flow in nanoporous structures based on a homogenization approach is described. Both, the models and the extension were developed in Task 4.1 to investigate electrolyte intrusion on the pore-scale using simulations. The report is structured as follows. After a short general introduction in Section 3, the Lattice Boltzmann software tools used and developed within the current project are introduced in Section 4. The different Lattice Boltzmann models and their parametrization are described in Section 5. Finally, validation concepts and preliminary results are given in Section 6.

2 Acronyms and abbreviations

BGK	Bhatnagar, Gross and Krook
CGM	Color-Gradient Method
GM	Grayscale Method
LB	Lattice Boltzmann
LBM	Lattice Boltzmann Method
MCSC	Multi-Component Shan-Chen Method
SC	Shan-Chen
SEI	Solid Electrolyte Interface
WP	Work Package

Horizon 2020
European Union Funding
for Research & Innovation

This project has received funding from
the European Union's Horizon 2020 research and innovation
programme under grant agreement No 875247

3 Introduction

An optimized electrolyte filling process affects both the battery production as well as the battery performance. From the economical point of view, the electrolyte filling process is time-consuming and expensive. Optimization of process parameters is often done on an empirical basis, which impedes adapting process parameters for new electrode types or cell types. From the electrochemical point of view, imperfect filling leads to a reduced effective ion conductivity as well as inhomogeneities in the solid electrolyte interface (SEI) [1] and the potential distribution. These effects may lead to a downgrade of the battery performance and favor degradation mechanisms.

Thus, the scope of work package 4 (WP4) is to investigate the influence of process parameters and material properties on the process duration, the degree of saturation, and the distribution of electrolyte in the electrode and the separator. Different models were developed and implemented to study structurally resolved filling processes using the Lattice Boltzmann method (LBM). The model will give a detailed insight into physical phenomena on the pore-scale and will be finally used to optimize the filling process.

4 Software Tools

In the current section, two different Lattice Boltzmann (LB) tools that are further developed and used within WP4 of DEFACTO are presented. Beside the features of both tools, also the advantages and disadvantages with respect to computational efficiency and future usability beyond the project term are discussed.

4.1 DLR Code

Within the past years, a LB solver has been developed at DLR. This in-house software tool is written in C++ and optimized for parallel execution on a single node using OpenMP. The tool is especially suited for simulating multi-phase phenomena based on the color-gradient method (CGM). So far, the DLR code has been mainly applied for studying the dynamics within gas-diffusion electrodes of lithium-air and zinc-air batteries as well as water flow in gas-diffusion layers of polymer electrolyte fuel cells [2].

The advantages of the DLR in-house software are the clarity, comprehensibility, and readability of the code which are preferential with respect to usability and further development of the code. The main disadvantage of the DLR in-house software is its restriction to single-node computation which makes it unfavorable for large-scale simulations as they are planned to be conducted on the longer term.

4.2 Palabos

Another LB simulation tool that is used and further developed within DEFACTO is the latest version of Palabos. It is an open-source project that is mainly developed under the auspices of the University of Geneva. The Palabos library is written in C++. It is highly optimized and parallelized using MPI. The software is freely available under the terms of an open-source AGPLv3 license. Palabos has so far been applied for a variety of scientific and engineering problems in the field of computational fluid dynamics. The studies based on Palabos have been published in more than 300 scientific publications [3].

The advantages of the Palabos are due to the modularity and computational efficiency of the software tool. Moreover, the Palabos library comes with a number of different models and boundary conditions already being implemented. Thus, it serves as a good starting position for further model development

Horizon 2020
European Union Funding
for Research & Innovation

This project has received funding from
the European Union's Horizon 2020 research and innovation
programme under grant agreement No 875247

and is preferential for large-scale simulations. There are no disadvantages of Palabos being worth mentioning which makes this tool favorable on the longer term.

5 Models and Simulation Setup

In the current section, the models and the simulation setup that are used to study the electrolyte filling process are described in detail. In all cases, the electrolyte filling is modeled as a multi-phase flow in which two immiscible phases – one representing the electrolyte and another representing a coexisting gas phase – are interacting via the corresponding surface tension. The wetting behavior of the solid electrode components is modeled via adhesive forces acting on both fluid phases. Beside a computationally efficient homogenization approach that is used to study the flow through the nanoporous binder structure, also the general simulation setup is described in the following.

5.1 Color-Gradient Method

In the CGM, the flow within each of the two immiscible phases, i.e. the liquid electrolyte and a coexisting gas phase, is described via separate Navier-Stokes equations. The contribution of the multi-phase flow, i.e. the interaction between both phases, enters via molecular interaction or collisions.

In the LB context, the Navier-Stokes equations for single-phase flow are typically modeled using the Bhatnagar, Gross and Krook (BGK) collision [4]:

$$f_i(x,t^*) = f_i(x,t) + \frac{1}{\tau}\left[f_i(x,t) - f_i^{eq}(x,t)\right] \tag{1}$$

It describes the streaming and the relaxation of a distribution function f_i towards its equilibrium, i.e. f_i^{eq}, within the relaxation time τ. The phases are typically distinguished with a the color-field ψ [5]

$$\psi(x,t) = \frac{\rho_{gas} - \rho_{liquid}}{\rho_{gas} + \rho_{liquid}}, \tag{2}$$

where ρ is the density of the corresponding phase at a location x and a time t.

The interfacial contribution is modeled in two subsequent collision steps [5]–[7]: (1) the perturbation that accounts for the interfacial tension and (2) the recoloring that accounts for the phase separation.

The perturbation step is given by the two-phase collision

$$f_i(x,t^{**}) = f_i(x,t^*) + \frac{A}{2}|\nabla\psi|\left[w_i\frac{(c_i\nabla\psi)^2}{|\nabla\psi|^2} - B_i\right], \tag{3}$$

where the parameter A determines the interfacial tension, w_i and B_i are specific lattice weights, and c_i is the discrete velocity along the direction i.

The recoloring step is

$$f_i^k(x + c_i\Delta t\,, \mathrm{t} + \Delta t) = \frac{\rho_k}{\rho_k + \rho_{\bar{k}}}\left(f_i^k(x,t^{**}) + f_i^{\bar{k}}(x,t^{**})\right) + \beta^{\mathrm{k}}\frac{\rho_k\rho_{\bar{k}}}{(\rho_k + \rho_{\bar{k}})^2}\cos(\phi_i)\, f_i^{eq}|_{u=0}, \tag{4}$$

Horizon 2020
European Union Funding
for Research & Innovation

This project has received funding from
the European Union's Horizon 2020 research and innovation
programme under grant agreement No 875247

where the indices k and $\bar{k}$ denote the phase and its corresponding counter phase, respectively. β is the interfacial thickness, that is positive for the gas phase and negative for the liquid phase. ϕ_i is the angle between the color gradient and the discrete velocity direction i.

In the CGM, the adhesive interaction between the solid and the fluid is modeled using a bounce-back scheme. The contact angle is adjusted by two different approaches: (1) assigning an effective density to the distribution functions at solid cells and (2) adjusting the unit normal to the interface in cells close to the solid boundary using a secant method [6], i.e. affecting the local color-gradient [6], [7]. The latter approach is mainly used in the following.

The pressure of each phase follows the ideal gas law and is determined as

$$p = c_s^2 \rho, \tag{5}$$

where c_s is the lattice speed of sound, i.e. $c_s = 1/\sqrt{3}$ in the current case.

The CGM is implemented in the DLR in-house software tool. As part of current project, it has also been implemented into Palabos. Using the CGM, mass and momentum of each phase are conserved locally in each cell. Moreover, it has the advantage, that the surface tension is independent of the relaxation parameter τ as well as the density ratio of the two phases. However, it becomes unstable for density ratio of about 30.

5.2 Multi-Component Shan-Chen Method

The multi-component Shan-Chen method (MCSC) is a different type of approach for modeling multi-phase flows in LBM. Similar to the CGM, in MCSC, the flow within each phase, is described via separate Navier-Stokes equations. Those are again determined as:

$$f_i(x + c_i\Delta t\ , \mathrm{t} + \Delta t) = f_i(x,t) + \frac{1}{\tau}\left[f_i(x,t) - f_i^{eq}(x,t)\right] \tag{6}$$

The contribution of the phase interaction enters via molecular interaction. In the MCSC, this is expressed bottom-up as a force F_{inter} that depends on the pseudopotential $\Psi = \rho$ which is a function of the phase density [8]:

$$F_{inter}^{k}(x) = -\Psi^{k}(x) \sum_{\bar{k}\neq k} G_{inter}^{k\bar{k}} \sum_i w_i\, \Psi^{\bar{k}}(x + c_i\Delta t) c_i \Delta t. \tag{7}$$

Here, $G_{inter}^{k\bar{k}}$ is a parameter that controls the strength of the interaction force and is therefore directly related to the interfacial tension. In a similar manner, the adhesive interaction between the solid and the fluid is modeled as a surface force acting on the k^{th} fluid component [8]:

$$F_{ads}^{k}(x) = -\Psi^{k}(x) \sum_{\bar{k}\neq k} G_{ads}^{k\bar{k}} \sum_i w_i\, s(x + c_i\Delta t) c_i \Delta t. \tag{8}$$

Horizon 2020
European Union Funding
for Research & Innovation

This project has received funding from
the European Union's Horizon 2020 research and innovation
programme under grant agreement No 875247

Here, $G_{ads}^{k\bar{k}}$ is a parameter that controls the strength of the interaction force and is therefore directly related to the wetting behavior of the fluid [8]. s is an indicator function that is equal to 1 or 0 for a solid or a fluid cell, respectively.

In the Shan-Chen forcing scheme which has been implemented in the Palabos code, both aforementioned force contributions (cf. Eqs. (7) & (8)) act on the equilibrium macroscopic velocity of each phase k which finally introduces the interfacial tension and wetting into the system [9]:

$$u_k^{eq} = \frac{\sum_k \left(\frac{\rho u}{\tau}\right)_k}{\sum_k \left(\frac{\rho}{\tau}\right)_k} + \frac{\tau_k F^k}{\rho_k} \tag{9}$$

Here, $F^k = F_{inter}^k + F_{ads}^k$ and the indices k and $\bar{k}$ denote the phase and its corresponding counter phase, respectively.

From Eq. (9) the macroscopic velocity of the fluid mixture can be determined as:

$$u^{macro} = \frac{\sum_k \left(\sum_i f_i^k c_i + \frac{F^k \Delta t}{2}\right)}{\sum_k \rho_k} \tag{10}$$

Different from the CGM (cf. Eq. (5)), using the MCSC, the pressure at a point x in space of each phase follows the ideal gas law and is determined as

$$p(x) = \sum_k c_s^2 \rho_k(x) + \frac{c_s^2 \Delta t^2}{2} \sum_{k,\bar{k}\neq k} G_{inter}^{k\bar{k}} \Psi^k(x) \Psi^{\bar{k}}(x), \tag{11}$$

where $c_s = 1/\sqrt{3}$ is the lattice speed of sound again.

The multi-component Shan-Chen method (MCSC) has been implemented into Palabos. In contrast to the CGM, when using the MCSC, the momentum of each phase is only conserved globally. Also, the surface tension is dependent on the relaxation parameter τ as well as the density ratio of the two phases. However, both disadvantages have only a minor effect for the current application. Instead, the MCSC is stable for a wider range of density and viscosity ratios which makes this method favorable for the applications in the current project.

5.3 Homogenization Approach

In the electrode structures studied in DEFACTO, pores on different length scales are considered. While the active material creates mesoscopic pores, an additional binder phase introduces nanoscopic pores. Thus, one of the goals in WP4 is to study electrolyte flow in such multi-scale porous structures using a computationally efficient way, i.e. without explicitly resolving the nanoscale. Instead, the influence of the nanopores on the electrolyte flow is mimicked using the so-called grayscale method (GM) [10], [11], which effectively adds a drag force to the fluid in nanoporous electrode regions. This method incorporates influences of fluid flow and of fluid-wall interaction by interpolating between the pure LB equation with BGK collision term (cf. Eq. (6)) and a bounce-back boundary condition. The corresponding interpolation factor is the solid fraction $n_s \in [0,1]$, where $n_s = 0$ corresponds to a purely fluidic behavior, while $n_s = 1$ corresponds to a purely solid behavior. The LB equation for the GM is:

Horizon 2020
European Union Funding
for Research & Innovation

This project has received funding from
the European Union's Horizon 2020 research and innovation
programme under grant agreement No 875247

$$f_i(x + c_i\Delta t\ , \mathrm{t} + \Delta t) = (1 - n_s)f_i(x,t) + (1 - n_s)\frac{1}{\tau}\left[f_i(x,t) - f_i^{eq}(x,t)\right] + n_s f_{\bar{\imath}}(x,t) \tag{12}$$

In the right most term, the index $\bar{\imath}$ is in the opposite direction to i and indicates that the distribution function to be added is also the opposite one. The only exception to this is the rest position $i = 0$, for which $\bar{\imath} = i = 0$.

The GM can basically be coupled to any LB model. Within DEFACTO, it is coupled to the MCSC described above (cf. Section 5.2). The basic adaptions that have to be made compared to the default MCSC, are that the discretized GM equation has to be solved (cf. Eq. (12)). In addition, the equilibrium velocity (cf. Eq. (9)) and the macroscopic velocity (cf. Eq. (10)) have to be supplemented by the interpolation factor n_s [11] as:

$$u_k^{eq} = (1 - n_s)\left[\frac{\sum_k \left(\frac{\rho u}{\tau}\right)_k}{\sum_k \left(\frac{\rho}{\tau}\right)_k} + \frac{\tau_k F^k}{\rho_k}\right], \tag{13}$$

$$u^{macro} = (1 - n_s)\frac{\sum_k \left(\sum_i f_i^k c_i + \frac{F^k \Delta \mathrm{t}}{2}\right)}{\sum_k \rho_k}. \tag{14}$$

5.4 Simulation Setup

One of the goals of WP4, is to determine capillary pressure-saturation curves of electrolyte filling processes using the LB simulation methods discussed above. The corresponding simulation setup is described in the following.

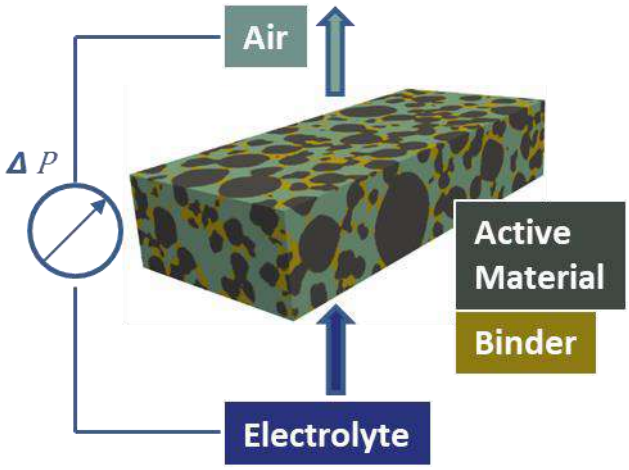

Figure 1: Schematic simulation setup as it is used for studying capillary pressure-saturation curves of electrolyte filling processes. Virtual NMC electrode structures consisting of active material (gray) and binder (yellow) are used. They are initially filled with air (green) and infiltrated with an electrolyte (blue). During the simulations the pressure difference ΔP between the inlet and the outlet is measured.

Horizon 2020
European Union Funding
for Research & Innovation

This project has received funding from
the European Union's Horizon 2020 research and innovation
programme under grant agreement No 875247

In Figure 1: Schematic simulation setup as it is used for studying capillary pressure-saturation curves of electrolyte filling processes. Virtual NMC electrode structures consisting of active material (gray) and binder (yellow) are used. They are initially filled with air (green) and infiltrated with an electrolyte (blue). During the simulations the pressure difference ΔP between the inlet and the outlet is measured. the simulation setup is shown schematically. Virtual NMC electrode structures consisting of active material and binder were generated stochastically [12] and were used for the studies presented in the current report. The structures have a size of 75 µm x 40 µm x 170 µm. They are discretized into approximately 6 million cells, which makes simulations computationally demanding. This is the main reason, while beside the DLR in-house code Palabos was considered especially for future large-scale simulations.

The wetting properties of both the active material and the binder can be adjusted. For the binder, in addition, the porosity can be adjusted. The structures are initially filled with air and infiltrated with an electrolyte during the simulation. Therefore, the pressure of the leaking phase, i.e. the air is kept constant, while the pressure of the penetrating phase, i.e. the electrolyte, is increased continuously. The pressure in each phase is controlled by applying corresponding inlet and outlet boundary conditions along one direction. Along the other directions periodic boundary conditions are applied. Finally, as a key observable, the pressure difference ΔP between the inlet, i.e. the electrolyte, and the outlet, i.e. the air, is measured and related to the corresponding state of saturation.

Saturation changes are usually highly sensitive to the capillary pressure for low and high values of the saturation, but rather insensitive for medium values. Thus, an adaptive inlet boundary condition was developed for the electrolyte intrusion. The new boundary condition automatically adjusts the capillary pressure based on a control loop. It has been implemented in both software tools, i.e. the DLR in-house code as well as Palabos.

6 Validation and Preliminary Results

In the current section, validation tests of the methods described in Section 5 as well as preliminary results of electrolyte filling processes are presented.

6.1 Wetting Behavior

The models for the wetting behavior, both for the CGM and the MCSC, are validated conducting sessile droplet simulations. Different setups are used for the simulations. All have in common, that a spherical liquid droplet which is initialized with the respective target contact angle is placed on a solid wall. The simulations differ by the target contact angle, the slope of the wall, and the radius of the droplet. The range of contact angles studied was [25, 155]°. Two different wall slopes {0, 30}° and two different radii {0.06, 0.10}mm were studied. Each simulation ran for 100,000 time steps to ensure that a steady state was reached.

Exemplary results, i.e. a snapshot from the simulation (top) and the contour line of the interface (bottom) determined using the CGM and the in-house tool are shown in Figure 2 and Figure 3.

Figure 2 shows a droplet on a plane solid wall with a target contact angle of 25°. Figure 3 shows a droplet on a sloped solid wall with a target contact angle of 40°. In total, the contacted angles determined from the simulations showed a good agreement with the corresponding target contact angle. Deviations were in a range of $\pm$ 2.5°.

Horizon 2020
European Union Funding
for Research & Innovation

This project has received funding from
the European Union's Horizon 2020 research and innovation
programme under grant agreement No 875247

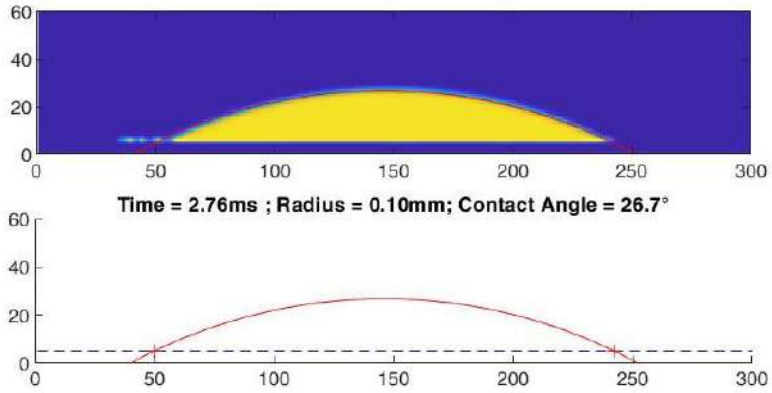

Figure 2: Sessile droplet with a radius of 0.10 mm on a plane solid wall with a target contact angle of 25°. Top: Snapshot of the simulation using the CGM. The liquid phase is depicted in yellow, and the gas phase is depicted in blue. Bottom: The red line is the contour line of the interface after post-processing. The blue dashed line represents the solid surface.

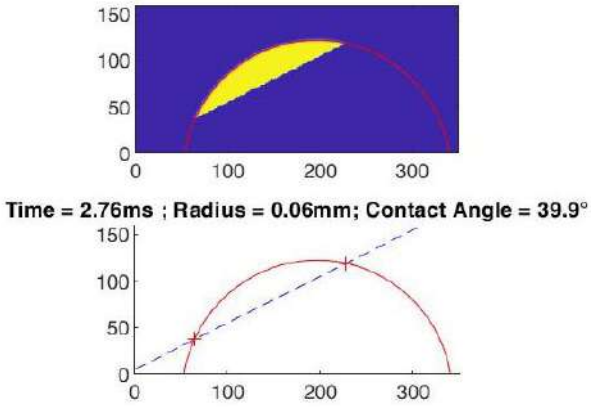

Figure 3: Sessile droplet with a radius of 0.06 mm on a sloped solid wall (slope = 30°) with a target contact angle of 40°. Top: Snapshot of the simulation using the CGM. The liquid phase is depicted in yellow, and the gas phase is depicted in blue. Bottom: The red line is the contour line of the interface after post-processing. The blue dashed line represents the solid surface.

Similar sessile droplet simulations for the MCSC have been set up and conducted with Palabos. The results agreed well with the following correlation from Huang et al. [8]:

$$cos\theta = \frac{G_{ads}^{\bar{k}k} - G_{ads}^{k\bar{k}}}{G_{inter}^{k\bar{k}} \left(\frac{\rho_k - \rho_{\bar{k}}}{2}\right)}, \tag{15}$$

where θ is the contact angle, G is a model parameter (cf. Eqs. (7) & (8)), ρ is the density, and the indices k and $\bar{k}$ denote the liquid phase and the gas phase, respectively.

6.2 Homogenization Approach

For validation purposes of the physical behavior of the coupled approach between GM and MCSC two-phase flow simulations around and through a nanoporous spherical particle have been conducted. Exemplary results are shown in Figure 4: Time evolution of a MCSC two-phase flow coupled with the GM. The two phases are a liquid (red) and a gas (blue). The GM is applied to a nanoporous spherical region in the center of the simulation domain. The flow direction is from the left to the right of the simulation domain.. There, a system that is initially filled with a gas (blue) is exposed to a pressure gradient that leads to an inflation with a liquid (red) which enters from the left. In the center of the

Horizon 2020
European Union Funding
for Research & Innovation

This project has received funding from
the European Union's Horizon 2020 research and innovation
programme under grant agreement No 875247

system a transparent nanoporous spherical particle is considered, to which the GM with $n_s = 0.5$ is applied. In the area surrounding this particle, the GM with $n_s = 0$ is applied, which is comparable to a purely fluidic flow represented by the Navier-Stokes equations.

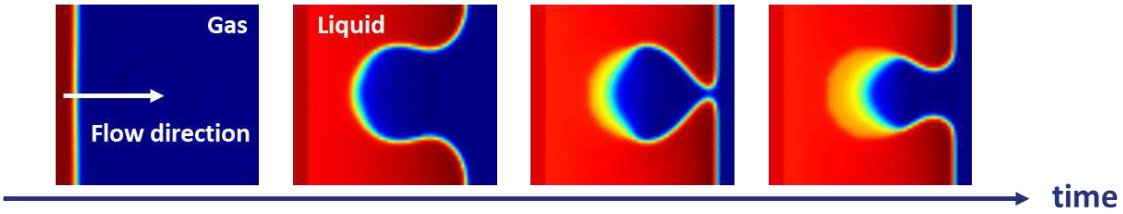

Figure 4: Time evolution of a MCSC two-phase flow coupled with the GM. The two phases are a liquid (red) and a gas (blue). The GM is applied to a nanoporous spherical region in the center of the simulation domain. The flow direction is from the left to the right of the simulation domain.

The results show, that the coupled approach between GM and MCSC reveals the basic physics of the problem investigated. Those are: (1) A stable two-phase flow with a distinct interface between the liquid and the gas is observed in all regions of the simulation domain. (2) The influence of the wetting, both at the surface of the nanoporous particle as well as in its inner region is modeled successfully. (3) Undisturbed, unrestrained, and therefore fast two-phase fluid flow is observed in the regions around the nanoporous particle. (4) Retarded two-phase fluid flow is observed through the nanoporous particle, i.e. in the center of the simulation domain, where in dependence on the solid fraction a drag force is applied to the fluid.

However, it was shown in the literature [10] that the GM model parameter n_s, i.e. the solid fraction, does not directly correspond to the porosity of the nanoporous material, i.e. the real solid fraction. Therefore, following the approach from Costa [13], permeability studies have been conducted to relate the permeability of a nanoporous material with a given solid fraction to its porosity. Results for different tortuosities τ are given in Figure 5.

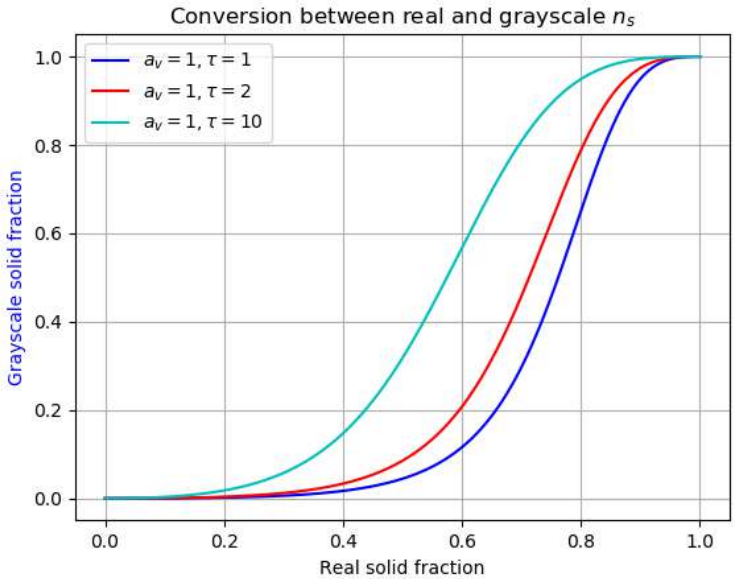

Figure 5: Correlation between the GM model parameter n_s, i.e. the solid fraction, and the porosity of the nanoporous material, i.e. the real solid fraction, given for different tortuosities τ.

Horizon 2020
European Union Funding
for Research & Innovation

This project has received funding from
the European Union's Horizon 2020 research and innovation
programme under grant agreement No 875247

Horizon 2020
European Union Funding
for Research & Innovation

This project has received funding from
the European Union's Horizon 2020 research and innovation
programme under grant agreement No 875247

6.3 Pressure-Saturation Behavior

The simulations of the capillary pressure-saturation behavior of electrodes during a filling process were conducted using the setup described in Section 5.4. For the preliminary study, for which the results are given in the following, different influencing factors were considered: (1) Porosity of the electrode, (2) content of the binder, (3) wetting behavior of the active material, and (4) wetting behavior of the binder. The porosity of the electrodes was varied in the range $\phi = \{50, 40, 30\}\%$, which corresponds to the structures {Ia, IIa, IIIa}. Most of the simulations were conducted without binder; only one simulation with a binder content of 14 volume-%, which corresponds to the structure Ib, was studied. For that simulation the GM with $n_s = 0.5$ was applied to the binder regions. The contact angle of the active material was varied in the range $\Theta_A = \{40, 60, 80\}°$. The contact angle of the binder was varied in the range $\Theta_B = \{20, 40, 60\}°$. The simulations of the results given in the following are based on the coupled approach between GM and MCSC and have been conducted using Palabos.

Figure 6 shows the influence of the porosity and the wetting behavior of the active material on the capillary pressure-saturation behavior. All three structures used here, which are Ia, IIa, and IIIa, solely consist of active material. The porosity ϕ of the structures and the contact angle Θ_A are given in the legend. All curves show a similar qualitative behavior. The main observations are: (1) The starting point of the saturation curves is hardly affected by the porosity. (2) At medium saturation, the filling process of structures with smaller porosity requires a larger pressure difference. (3) The final degree of saturation varies with respect to the porosity. The saturation is smaller for a smaller porosity. (4) The lower the contact angle is, the smaller is the pressure difference and the larger is the degree of saturation.

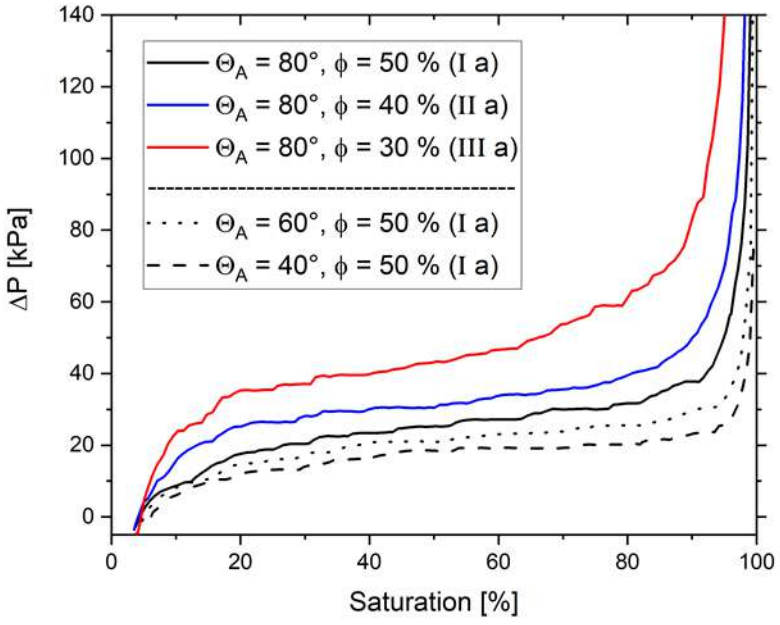

Figure 6: Capillary pressure-saturation curves under the influence of the porosity and the wetting behavior of the active material. The porosity ϕ of the structures and the contact angle Θ_A are given in the legend.

Figure 7 shows the influence of the binder and the corresponding wetting of the binder on the capillary pressure-saturation behavior. Results are compared for the structures Ia and Ib. It it is observed that

Horizon 2020
European Union Funding
for Research & Innovation

This project has received funding from
the European Union's Horizon 2020 research and innovation
programme under grant agreement No 875247

inducing a strongly wetting binder structure in general leads to a reduction of the pressure difference and a shift of the starting point of the pressure saturation curves to the right. The latter increases with a decreasing contact angle. Thus, inducing a wetting binder seems to be favorable for an optimization of the filling process.

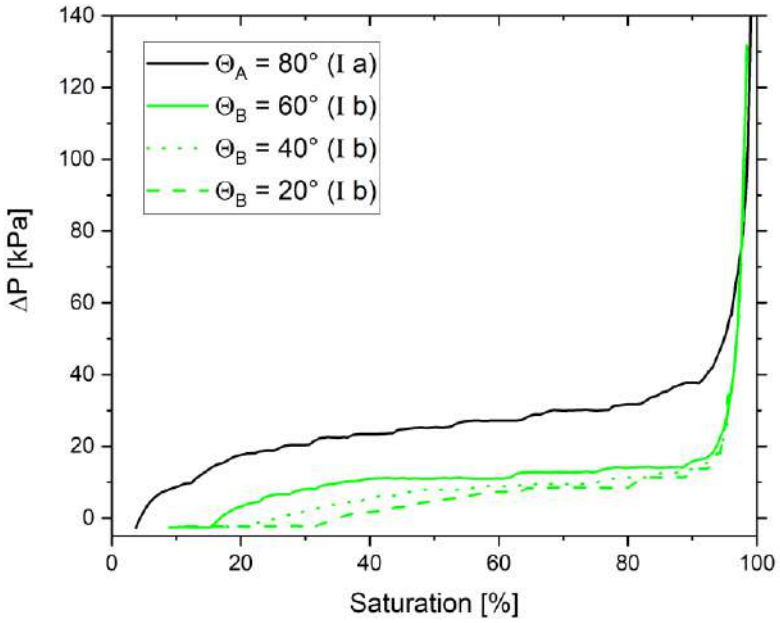

Figure 7: : Capillary pressure-saturation curves under the influence of the binder and the corresponding wetting of the binder. The contact angle of the active material is $\Theta_A = 80°$ in all cases. For the green curves, the binder content is 14 volume-% in all cases. The corresponding contact angle of the binder Θ_B is varied and given in the legend.

7 Conclusions

The current report with respect to the deliverable D4.1 provides an overview of the software tools, models, validation approaches, and preliminary results that have been implemented, used, and obtained in the research within WP4. The report contains the most important models and equations that are necessary to study electrolyte filling processes using LBM. Beside the models, also the simulation setup is described in detail. Most of the physical phenomena modeled in the current context have been validated. Stable solutions were obtained that are in good agreement with results from the literature. The model was shown to give a first interesting insight into the influence of structural and physico-chemical properties on the electrolyte filling process. Further calibration and model extension, where necessary, are conducted. Still, the current results lay the foundation for the upcoming work in WP4.

Horizon 2020
European Union Funding
for Research & Innovation

This project has received funding from
the European Union's Horizon 2020 research and innovation
programme under grant agreement No 875247

8 References

[1] C. Sauter, R. Zahn, and V. Wood, "Understanding Electrolyte Infilling of Lithium Ion Batteries," *J. Electrochem. Soc.*, vol. 167, no. 10, p. 100546, 2020, doi: 10.1149/1945-7111/ab9bfd.

[2] T. Danner, S. Eswara, V. P. Schulz, and A. Latz, "Characterization of gas diffusion electrodes for metal-air batteries," *J. Power Sources*, vol. 324, pp. 646–656, 2016, doi: 10.1016/j.jpowsour.2016.05.108.

[3] J. Latt *et al.*, "Palabos: Parallel Lattice Boltzmann Solver," *Comput. Math. with Appl.*, vol. 81, pp. 334–350, Jan. 2021, doi: 10.1016/j.camwa.2020.03.022.

[4] P. L. Bhatnagar, E. P. Gross, and M. Krook, "A Model for Collision Processes in Gases. I. Small Amplitude Processes in Charged and Neutral One-Component Systems," *Phys. Rev.*, vol. 94, no. 3, pp. 511–525, May 1954, doi: 10.1103/PhysRev.94.511.

[5] H. Liu, A. J. Valocchi, and Q. Kang, "Three-dimensional lattice Boltzmann model for immiscible two-phase flow simulations," *Phys. Rev. E - Stat. Nonlinear, Soft Matter Phys.*, vol. 85, no. 4, pp. 1–14, 2012, doi: 10.1103/PhysRevE.85.046309.

[6] S. Leclaire, A. Parmigiani, O. Malaspinas, B. Chopard, and J. Latt, "Generalized three-dimensional lattice Boltzmann color-gradient method for immiscible two-phase pore-scale imbibition and drainage in porous media," *Phys. Rev. E*, vol. 95, no. 3, p. 033306, Mar. 2017, doi: 10.1103/PhysRevE.95.033306.

[7] S. Leclaire, K. Abahri, R. Belarbi, and R. Bennacer, "Modeling of static contact angles with curved boundaries using a multiphase lattice Boltzmann method with variable density and viscosity ratios," *Int. J. Numer. Methods Fluids*, vol. 82, no. 8, pp. 451–470, Nov. 2016, doi: 10.1002/fld.4226.

[8] H. Huang, D. T. Thorne, M. G. Schaap, and M. C. Sukop, "Proposed approximation for contact angles in Shan-and-Chen-type multicomponent multiphase lattice Boltzmann models," *Phys. Rev. E - Stat. Nonlinear, Soft Matter Phys.*, vol. 76, no. 6, pp. 1–6, 2007, doi: 10.1103/PhysRevE.76.066701.

[9] X. Shan and H. Chen, "Simulation of nonideal gases and liquid-gas phase transitions by the lattice Boltzmann equation," *Phys. Rev. E*, vol. 49, no. 4, pp. 2941–2948, Apr. 1994, doi: 10.1103/PhysRevE.49.2941.

[10] S. D. C. Walsh, H. Burwinkle, and M. O. Saar, "A new partial-bounceback lattice-Boltzmann method for fluid flow through heterogeneous media," *Comput. Geosci.*, vol. 35, no. 6, pp. 1186–1193, 2009, doi: 10.1016/j.cageo.2008.05.004.

[11] G. G. Pereira, "Grayscale lattice Boltzmann model for multiphase heterogeneous flow through porous media," *Phys. Rev. E*, vol. 93, no. 6, pp. 1–14, 2016, doi: 10.1103/PhysRevE.93.063301.

[12] J. Feinauer, T. Brereton, A. Spettl, M. Weber, I. Manke, and V. Schmidt, "Stochastic 3D modeling of the microstructure of lithium-ion battery anodes via Gaussian random fields on the sphere," *Comput. Mater. Sci.*, vol. 109, pp. 137–146, 2015, doi: 10.1016/j.commatsci.2015.06.025.

[13] A. Costa, "Permeability-porosity relationship: A reexamination of the Kozeny-Carman equation based on a fractal pore-space geometry assumption," *Geophys. Res. Lett.*, vol. 33, no. 2, pp. 1–5, 2006, doi: 10.1029/2005GL025134.

Horizon 2020 European Union Funding for Research & Innovation

This project has received funding from the European Union's Horizon 2020 research and innovation programme under grant agreement No 875247